Proton Transfer in Homodimers of Carboxylic Acids: The Rotational Spectrum of the Dimer of Acrylic Acid

Gang Feng,[‡] Laura B. Favero,[§] Assimo Maris,[‡] Annalisa Vigorito,[‡] Walther Caminati,*[‡] and Rolf Meyer[⊥]

[‡] Dipartimento di Chimica "G. Ciamician", University of Bologna, Via Selmi 2, I-40126 Bologna, Italy
[§] Consiglio Nazionale delle Ricerche, Istituto per lo Studio dei Materiali Nanostrutturati (CNR-ISMN), via P. Gobetti 101, I-40129 Bologna, Italy
[⊥] Sonnenbergstrasse 18, CH-5621 Zufikon, Switzerland

 Ⓢ *Supporting Information*

ABSTRACT: The dimer of acrylic acid can exist in two forms, depending on the *entgegen* or *zusammen* orientations of the two allyl groups. The latter one (*zusammen*) has a permanent value of the μ_b dipole moment component, which allowed measuring its pulsed jet Fourier transform microwave (MW) spectrum. From the tunneling splitting, originating in the concerted proton transfer of the two carboxylic hydrogen atoms and measured for four isotopologues of such a bimolecule, we could determine the barrier and dynamics of the proton transfer.
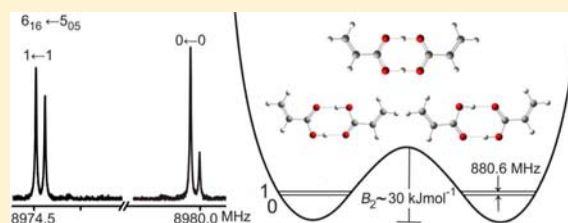
INTRODUCTION

Pairs of carboxyl groups bind cooperatively together, since both units act as proton donor and acceptor, forming a large eight-membered ring containing two hydrogen bonds. Such a kind of hydrogen bonding is the strongest one found within neutral species, with the monomers held together by more than 60 kJ/mol. Gilli suggested to explain such a "strong" interactions in terms of a resonance assisted hydrogen bond model.[1]

Another interesting feature of these bimolecules is that the concerted double transfer of the protons corresponds to a motion with a double minimum potential (Figure 1), which can generate tunneling doubling within spectroscopic studies, useful to determine the barrier to the proton transfer.
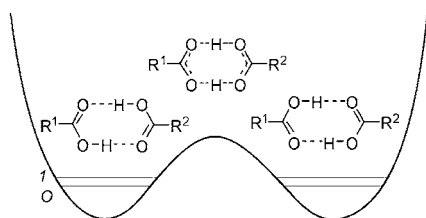
Figure 1. Proton tunneling and potential energy function to the proton transfer in carboxylic acid bimolecules.

At a first sight, homodimers do not possess a dipole moment, so that they cannot be studied by microwave spectroscopy (MW).

However, admirable spectroscopic results have been obtained so far on the homodimers of carboxylic acids with other high-resolution techniques. Among them, a rotationally resolved laser-induced fluorescence (LIF) investigation of the dimer of benzoic acid[2] allowed for the tunneling effects to be measured.

LIF generally requires a chromophore, so that the homodimers of simpler carboxylic acids have been investigated with other high-resolution methods such as femtosecond degenerate four-wave mixing and Raman spectroscopy.

These methods supplied information, such as tunneling splittings in the ground and vibrationally excited states, on formic acid[3−9] and acetic acid[10] homodimers.

This kind of complex has been investigated also by MW spectroscopy. Carboxylic acid dimers were early observed with low-resolution MW spectroscopic methods by Costain in 1961[11] and Bellot and Wilson in 1975.[12] Then Bauder and co-workers provided detailed supersonic-jet FTMW analyses for some carboxylic acid bimolecules: the structures of $CF_3COOH\cdots HCOOH$ and $CF_3COOH\cdots CH_3COOH$ have been determined through the analyses of the rotational spectra of several isotopologues.[13] For the latter complex, also the V_3 barrier to internal rotation of the methyl group was determined. Antolinez et al. reported the MW spectrum of the trifluoroacetic acid−cyclopropanecarboxylic acid bimolecule.[14] In none of these cases, doubling of the rotational transitions attributable to a double proton transfer tunneling is observed. The proton transfer would have required, indeed, a simultaneous internal rotation of the heavy CF_3 top to reach an equivalent potential energy minimum. The resulting small reduced constants of the motion quenched the tunneling effects.

Only recently, doubling related to the proton transfer have been observed on the FTMW spectrum of the formic acid−propriolic acid dimer, but it was soon realized that there were errors in line assignments, and these were corrected,[15b] yielding

an accurate tunneling frequency. A much more extensive set of measurements for this complex was published over a year ago.[16]

In 2011, Howard and collaborators published the results of their investigation on the formic acid−acetic acid bimolecule.[17] There, the double proton transfer motion is coupled—in order to reach an equivalent minimum—with a 60° internal rotation of the methyl group. The problem is similar to that encountered in the case of proton transfer in methylmalonaldehyde.[18] Howard conducted a superb analysis of the two-dimensional (2D) problem, but its complexity made it difficult to obtain from the determined splittings a precise and unique value of the barrier to the proton transfer.

In case of dimers without additional motion with respect to the coupled proton transfer, it would be more direct to estimate the potential energy surface.

It has been claimed that "only hetero dimers can be studied by microwave spectroscopy".[17] Actually, there are at least three cases in which homodimers of carboxylic acids can give a rotational spectrum: (i) homodimers with a dipole moment induced by asymmetric isotopic substitution, as observed so far only for monomers, such as in the case of benzene-d1;[19] (ii) homodimers of homochiral carboxylic acids; (iii) homodimers of different conformers of the same carboxylic acid.

We will consider here case (iii), in relation to the dimer of acrylic acid (AA). AA has been investigated by MW spectroscopy, and the rotational spectra of two almost isoenergetic forms, shown in Figure 2, have been assigned.[20]
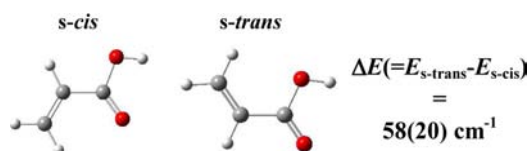

Figure 2. Two stable conformers of acrylic acid.

The dimerization of acrylic acid produces four different bimolecules, as shown in Figure 3. They can be divided into two pairs, where the two forms are converted to each other through a double proton exchange. The pair *cis···cis/trans···trans* consists of two different nonpolar dimers, each having a different energy. The pair *cis···trans/trans···cis* consists of two equivalent polar dimers, each with the same energy.
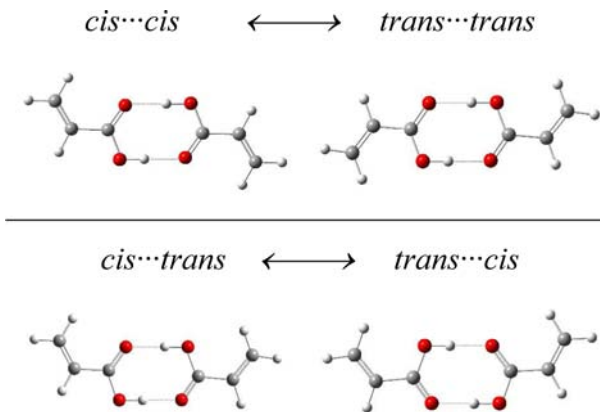

Figure 3. Homoconformational dimers of AA (*s-cis···s-cis*, *s-trans···s-trans*) are nonpolar, while heteroconformational dimers (*s-cis···s-trans*, *s-trans···s-cis*) are polar molecules.

For this form it is then possible to measure the rotational spectrum, and tunneling effects are expected. For this reason we decided to analyze the rotational spectrum of this bimolecule.

EXPERIMENTAL SECTION

A commercial sample of acrylic acid was supplied by Aldrich and used without further purification.

The spectrum was recorded with the Fourier transform[21] Bologna spectrometer (6−18.5 GHz). It is a COBRA-type[22] one, described elsewhere.[23] A gas mixture of approximately 2% of acrylic acid in helium at a total pressure of 3×10^5 Pa was expanded through the solenoid valve (General Valve, series 9, nozzle diameter 0.5 mm) into the Fabry-Pérot cavity. The frequencies were determined after Fourier transformation of the 8k data points time domain signal, recorded with 100 ns sample intervals. Each rotational transition is split by Doppler effect, enhanced by the molecular beam expansion in the coaxial arrangement of the supersonic jet and resonator axes. The rest frequency is calculated as the arithmetic mean of the frequencies of the Doppler components. The estimated accuracy of frequency measurements is better than 3 kHz, and lines separated by more than 7 kHz are resolvable.

RESULTS AND DISCUSSION

Theoretical Calculations. Before searching for the spectrum, we performed B3LYP/6-311++G** theoretical calculations[24] to estimate the relative energies of the dimers and of the transition state and to predict the values of the spectroscopic parameters. The shapes of the three conformers are shown in Figure 3, and the numerical results are reported in Table 1. There, ΔE and ΔE_0, are the energies relative to the

Table 1. Calculated (B3LYP/6-311++G) Values of Relative Energies, Dissociation Energies, Spectroscopic Constants and Dipole Moment Components of the Three Conformations of $(AA)_2$**

	cis···cis	trans···trans	cis···trans
ΔE/kJ mol^{-1}	0^a	2.13	1.09
ΔE_0/kJ mol^{-1}	0^b	1.81	1.02
D_e/kJ mol^{-1}	67.2	68.0	67.5
D_0/kJ mol^{-1}	62.0	63.1	62.4
B_2/kJ mol^{-1}	29.5	27.4	27.9
A/MHz	4508	4888	4260
B/MHz	498	489	502
C/MHz	448	445	449
D_J/kHz	0.02	0.02	0.02
D_{JK}/kHz	0.00	−0.02	−0.05
D_K/kHz	2.26	1.95	2.73
d_1/Hz	−2.07	−1.84	−2.47
d_2/Hz	−0.14	−0.10	−0.17
μ_a/D	0	0	−0.02
μ_b/D	0	0	0.90

^{a}Absolute value: −534.532034 E_h. ^{b}Absolute value: −534.395795 E_h.

more stable adduct, with and without zero point energy corrections. D_e and D_0 are the corresponding dissociation energies, while B_2 is the barrier to the proton transfer.

Geometry optimization and harmonic frequencies calculations were also run using the counterpoise method which takes into account the basis-set superposition error (BSSE) correction.[25] Whereas the resulting structural changes are negligible, the zero-point energy corrected dissociation energy values decrease to $D_0 = 58.6$, 59.6, and 59.0 kJ mol^{-1} for the *cis···cis*, *trans···trans*, and *cis···trans* conformers, respectively. It is

worthwhile noting that the *cis⋯cis* and *trans⋯trans* species have a C_{2h} symmetry, while the *cis⋯trans* form belongs to the C_s group. However, feasible operations such as the internal proton transfer will increase the symmetry of the bimolecules, so that in the case of a low barrier to proton transfer it will effectively be C_{2v} for the *cis⋯trans* conformer at the saddle point.

The geometries of the optimized structures and the list of the energy and spectroscopic parameters obtained with the BSSE corrections are given in the Supporting Information.

The polar species is drawn again in Figure 4, in order to introduce some labels used through the text. First of all, with
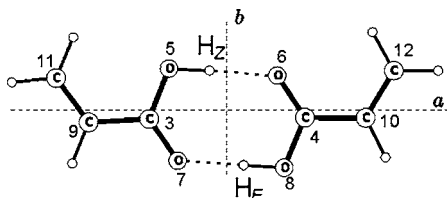

Figure 4. Atom labeling of the polar form of $(AA)_2$.

respect to the general case of Figure 1, the two hydroxyl hydrogens are different from each other. We label them as *zusammen* (Z) or *entgegen* (E) the one close and the one far away from the two allyl groups, respectively.

Rotational Spectrum. We report the rotational spectra of the most abundant species (normal species), and of the OD mono- and dideuterated species, prepared by mixing the sample with D_2O. For simplicity, we will label the normal and deuterated species as HH, DH, HD, and DD, where the first and second positions of the capital letter indicate the isotopic (H or D) nature of the Z and E hydrogens, respectively. We investigated first the spectrum of the normal (HH) species.

This bimolecule has a predominant μ_b dipole component, so that we started the search of its μ_b-type transitions. We observed and assigned first transitions of the type $(J + 1)_{1,(J+1)} \leftarrow J_{0,J}$, with J from 3 to 7. Each transition was split into two lines due to the proton tunneling, and each of them appeared as a doublet according to the Doppler effect. Then some $K_a = 2 \leftarrow$

1 transitions and some *Q*-branch transitions were also measured. All transitions have been fitted simultaneously with a coupled Hamiltonian using the Pickett set of programs.[26] We used the following expressions:

$$H = \sum_i H_i^R + H^{CD} + H^{int} \tag{1}$$

where $i = 0,1$ and

$$H^{int} = \Delta E_{01} + F_{ab} \times (P_a P_b + P_b P_a) \tag{2}$$

where H_i^R represents the rotational Hamiltonian for the state i. H^{CD} accounts for the centrifugal distortion corrections, corresponding to the I^r representation of Watson's "S" reduced Hamiltonian,[27] assumed to be the same for both states. ΔE_{01} is the energy difference between the $v = 0$ and $v = 1$ tunneling states. F_{ab} is the rotation–vibration coupling parameter between the two states. The spectroscopic constants obtained are reported in the first column of data of Table 2. A statistical weight of about 9/7 was observed in favor of the transitions with the starting rotational level having an odd value $(K_a + K_c)$ for $v = 0$, and vice versa for $v = 1$.

We investigated then the DH, HD, and DD species. Since their ΔE_{01} splittings were much smaller than those of the HH species, it was difficult to fit simultaneously the ΔE_{01} and the F_{ab} parameters. However, according to Pickett,[28] we could calculate these values from the rotation of the principal axes system to the reduced Eckart axes system.[29] We found that F_{ab} was slightly decreasing for the deuterated species with respect to the normal species. Thus, we fixed the fits in the F_{ab} parameters to the values scaled according to these indications.

The results of the three fits (including scaled F_{ab} values) are given in Table 2. In the case of the deuterated species, the hyperfine structure due to the quadrupole effects of deuterium ($I = 1$) has been partially resolved. The obtained quadrupole coupling constants are also reported in Table 2. They are in good agreement with the *ab initio* values, $\chi_{aa} = 0.20$, $\chi_{bb} = -0.09$ and $\chi_{cc} = -0.11$ MHz, respectively, for both D_Z and D_E atoms.

Not all the dipole moment components yield by *ab initio* computations can be used in the usual way. For example in this

Table 2. Experimental Spectroscopic Constants of the Observed Isotopologues of $(AA)_2$ (S Reduction, I^r Representation)

	HH	DH	HD	DD
A_0/MHz	4235.871(2)^a	4207.2469(2)	4171.29706(9)	4142.9926(2)
A_1/MHz	4235.850(2)	4207.2450(2)	4171.29347(9)	4142.9921(2)
B_0/MHz	508.874(1)	507.8477(3)	507.95476(7)	507.0070(1)
B_1/MHz	508.866(1)	507.8568(3)	507.95412(7)	507.0072(1)
C_0/MHz	454.2853(2)	453.1437(3)	452.8074(1)	451.7206(8)
C_1/MHz	454.2793(2)	453.1420(3)	452.80468(7)	451.7253(7)
D_J/kHz	0.0194(4)	[0.0194]^b	[0.0194]	[0.0194]
D_{JK}/kHz	−0.051(3)	[−0.0517]	[−0.0517]	[−0.0517]
D_K/kHz	2.2(3)	[2.215]	[2.215]	[2.215]
d_1/kHz	−0.0014(2)	[−0.00142]	[−0.00142]	[−0.00142]
ΔE_{01}/MHz	880.6(9)	117.0(9)	117.1(9)	31(4)
F_{ab}/MHz	47.43(6)	{47.03}^{c}	{46.73}	{46.43}
$\chi_{aa}(Z)$/MHz		0.177(2)		0.179(4)
$\chi_{aa}(E)$/MHz	−	−	0.176(1)	0.179(4)
$\chi^-(E)$/MHz^d	−	−	0.023(2)	
σ/kHz^e	2.2	3.0	3.3	3.4
N^f	82	94	92	100

^{a}Error in parentheses in units of the last digit. ^{b}Values in brackets have been kept fixed to the corresponding values of the HH species. ^{c}Values in braces fixed at the scaled values; see text. $^d\chi^- = \chi_{bb} - \chi_{cc}$. ^{e}Root-mean-square deviation of the fit. ^{f}Number of lines in the fit.

case, the μ_a component is antisymmetric with respect to the vibrational coordinate so the rotational transitions controlled by this component are forbidden within the same vibrational state, but allowed as vibrational–rotational transitions between the doublet states. This allows the determination of the energy spacing between doublets directly. In this case, however, it is not possible to observe these direct transitions due to the low value of the μ_a component. Anyway, thank to the interactions between rotational levels in the two adjacent tunneling states, we could determine the ΔE_{01} values for all isotopologues with good precision, rarely achieved with other techniques.

In principle, from the rotational constants of the deuterated species, one could locate the r_s positions[30] of the two hydroxyl hydrogens. However, the fact that these two atoms undergo motions of large amplitude and that the Ubbelohde effect[31,32] produces a shrinkage of the O···O distances between the two oxygen atoms involved in each hydrogen bond leads to meaningless values. Actually, the geometries calculated *ab initio* for the equivalent minima are not a good specification of the structure of the molecule, contrary to what a standard reader in chemistry may think. The real way to state the structure of these systems is to specify the potential energy surface and the minimum energy pathway for the proton transfer motion. We will elucidate this aspect better in the following section.

Model Calculations for Proton Transfer. From the measured tunneling splittings it is, in principle, possible to determine the barrier to the concerted double proton transfer.

The situation is much more complex, however, than for the familiar determination of a barrier hindering the internal rotation of a methyl group. In this latter case the motion in question is well described by rigid frame–rigid top model, as its vibration is usually at the lowest frequency and therefore well separated from the other molecular vibrations. By contrast, proton transfer is a fast motion at high energy that involves breaking and forming strong bonds, and it depends on the cooperative rearrangement of slowly vibrating modes of heavy nuclei. A well-known example is the proton transfer in malonaldehyde. For this system it has not been possible so far to derive the barrier height directly from the experimental data, but a large amount of properties obtained *ab initio* on a grid along the minimum energy path (MEP) have been needed to devise a full dimensional model able to reproduce a set of observed properties.[33]

Nevertheless, a simpler treatment of the most relevant molecular motions still seems to be desirable for the interpretation of spectroscopic data. We therefore tried to restrict the *ab initio* results to the stationary points of the potential energy surface and to use the structural changes obtained when going from the saddle point to either equilibrium configuration to define two modes of motion that are expected to be coupled most with the proton transfer. The simultaneous transfer of the proton pair is described by the displacement along the line connecting the carboxylic carbons from their midpoint. After dividing by the displacement at equilibrium one obtains the more useful reduced variable x. We note that the structure of the *cis–trans* acrylic acid dimer at the saddle point ($x = 0$) has C_{2v} symmetry and that upon reaching equilibrium at $x = \pm 1$ the structural parameters (bond lengths and angles) change by amounts $\Delta S_t(\pm 1)$ that are predicted *ab initio*. ΔS_t involves a component $[\Delta S_t(1) - \Delta S_t(-1)]/2$ of symmetry species B_1 and a component $[\Delta S_t(1) + \Delta S_t(-1)]/2$ of species A_1. We associate these components with reduced variables y_1 and y_2 that are assumed to follow the MEP if $y_1 = x$

and $y_2 = x^2$. More generally, the variables (x, y_1, y_2) refer to a planar 3D system[34] where the deviations from the MEP, $y_1 - x$ and $y_2 - x^2$, are displacements of the virtual modes that are used as representatives for the larger set of vibrations interacting with the proton transfer. The variable y_1 describes the B_1-type heavy atom motions, which are dominated by changes of CO bond lengths and C–CO_2 rocking angles, while the variable y_2 combines a large change of the distance between the two monomer units with several smaller A_1 type displacements. The potential surface assumed as

$$V(x, y_1, y_2) = s(x)\{B_2(1 - x^2)^2 + [f_1/s(1)](y_1 - x)^2$$
$$+ [f_2/s(1)](y_2 - x^2)^2\} \qquad (3)$$

involves a shape function $s(x)$ that ensures an asymptotic approach, along the MEP, to the dissociation energy D_0 and allows one to modify the barrier width by a factor w_b.

$$s(x) = 1/[1 + w_b(B_2/D_0)^{1/2}x^2 + (B_2/D_0)x^4] \qquad (4)$$

D_0 as well as the barrier B_2 can usually be obtained *ab initio*, whereas the force constant factors $f_i = k_i/2$ ($i = 1,2$) as well as the factor w_b are difficult to predict and should therefore rather be treated as parameters to be assumed or adjusted.

The proton motion in a deep double minimum potential involves high zero-point vibrational energy and is hence much faster than the heavy atom modes. A study by Manz et al.[35] for a prototype of coupled hydrogenic and heavy atom motion suggests an adiabatic approach, similar to the one applied to electronic and nuclear motion.

Using methods developed for flexible molecules[36] we therefore calculate energy levels of the proton motion (x) that depend parametrically on y_1 and y_2 in order to obtain the 'protonic' contribution to the potential energy of the y_1 and y_2 vibrations. For a symmetric reference system ($y_1 = 0$, $y_2 = 1$) the levels are grouped into tunneling doublets E_{n+}, E_{n-}. Therefore, we expect for each n two surfaces with avoided crossing that are to be converted into crossing surfaces by referring to a 'left' and 'right' localized basis $[\langle\phi_{nL}|, \langle\phi_{nR}|]$. In this representation we get $E_{nL} = E_{nR} = E_n$ and the interaction $W_n = (E_{n+} - E_n)/2$. For ($y_1 \neq 0$, $y_2 = 1$) the elements of the reference, $E_n|\phi_{nL}\rangle\langle\phi_{nL}|$, are to be complemented by the elements of the potential energy difference,

$$|\phi_{mL}\rangle\langle\phi_{mL}|V(x, y_1, 1) - V(x, 0, 1)|\phi_{nL}\rangle\langle\phi_{nL}| \qquad (5)$$

in order to obtain, after diagonalization, the surface point $E_{1L}(y_1,1)$ and the expansion coefficients $U_{nL,1L}$ for the lowest state $\phi_{1L}(x; y_1,1)$ at $y_1 \neq 0$ with respect to the reference states $\phi_{nL}(x; 0,1)$. The corresponding point on the R surface, $E_{1R}(y_1,1)$ is found similarly. Then the tunnel interaction for the lowest vibrational state of the transfer motion is obtained as $W(y_1,1) = \Sigma_n U_{nL,1L} W_n(0,1) U_{nR,1R}$. In the same way the y_2-dependent functions $E_{1L}(0,y_2)$, $E_{1R}(0,y_2)$ and $W(0, y_2)$ are calculated. To simplify the computations the complete functions $F(y_1,y_2)$ defining the two potential energy surfaces and the tunnel interaction function ($F = E_{1L}, E_{1R}, W$) are approximated by the one-dimensional profiles as

$$F(y_1, y_2) = F(y_1, 1) + F(0, y_2) - F(0, 1) \qquad (6)$$

This means that we neglect kinetic energy interactions between the coordinates x, y_1, and y_2, and it makes it possible to calculate the 2D wave functions for the heavy atom motions as products of 1D factors such as, $\chi_L(y_1, y_2) = \chi^{(1)}_L(y_1) \chi^{(2)}_L(y_2)$,

where $\chi^{(1)}_L$ is obtained as the lowest state of the y_1 motion with the potential energy profile $E_{1L}(y_1,1)$ and $\chi^{(2)}_L$ as the lowest state of the y_2 motion with the potential energy profile $E_{1L}(0,y_2)$. The tunnel interaction in the vibrational ground state is then given by

$$W_{gs} = \langle \chi_L(y_1,y_2)|W(y_1,y_2)|\chi_R(y_1,y_2)\rangle \qquad (7)$$

and the respective tunneling splitting by $\Delta E = -2W_{gs}$.

As eqs 3 and 4 involve five parameters, it is clear that their values cannot be determined from the available experimental data alone. Presumably, we have fixed the least important one, $D_0 = 5216$ cm^{-1}, at the B3LYP result. Then, with different choices of fixed values for f_1 and f_2, the barrier B_2 and the barrier width parameter w_b were adjusted to fit the observed splittings for the HH, DH, HD, and DD species, while expecting the barrier to remain in the range of the *ab initio* values 2328 cm^{-1} (B3LYP) and 2723 cm^{-1} (MP2). The parameter w_b affects the width of the barrier, a property relevant to reproduce the ratio of the splittings deuterated to the parent species.

Table 3 shows the results obtained with a set of parameters that could be a plausible interpretation of the data. The chosen

Table 3. Results of the Model Calculations

	Tunneling Splittings	
	Obs	Calc
ΔE_{01}(HH)/MHz	880.6(6)[a]	880.5
ΔE_{01}(DH)/MHz	117.0(9)	118.8
ΔE_{01}(HD)/MHz	117.1(9)	115.2
ΔE_{01}(DD)/MHz	30(10)	21.4
	Parameters	
B_2/kJ·mol^{-1} = 29.7(18)	$w_b = 0.90$[b]	
f_1/cm^{-1} = 220[c]	f_2/cm^{-1} = 60[c]	

[a]Errors in parentheses are expressed in units of the last digit. [b]Shape function parameter. [c]Assumed, see text.

values $f_1 = 220$ cm^{-1} and $f_2 = 60$ cm^{-1} yield the local vibrational ground states at the energy of 549 cm^{-1} and fundamental frequencies of 125 cm^{-1} and 41 cm^{-1} for the representative y_1 and y_2 vibrations, respectively. As may be expected from eq 3, an increase in f_1 and/or f_2 will draw the system closer to the MEP and thus increase the effective mass of the resulting transfer motion. Therefore a lower barrier will be needed to offset the shrinking of the tunnel splittings. This is shown in Table 3S of the Supporting Information, that also led us to estimate the uncertainty of the barrier to proton transfer at 150 cm^{-1}. A diagram of the obtained potential energy function is shown in Figure 5.

The barrier to proton transfer appears consistent with the *ab initio* value (see Table 1) but is quite lower than the tentative
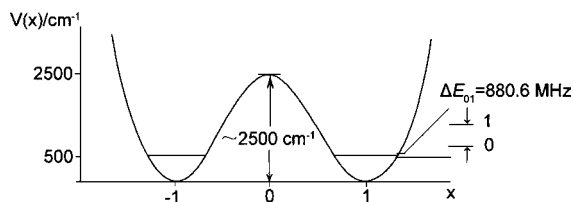
Figure 5. Diagram of the obtained potential energy function to the proton transfer in $(AA)_2$.

values calculated from the spectroscopic data in some cases (see Table 4). As to the value for the benzoic acid dimer, the authors give the $B_2 = 6224$ cm^{-1} and report in parentheses (7.45 kJ/mol), but it should be 74.5 kJ/mol, exaggeratedly high.

Table 4. Barriers to Proton Tunneling As Estimated from the Experimental Spectroscopic Data for Some Carboxylic Acid Bimolecules

	ΔE_{01}/MHz	B_2/cm^{-1}	ref
$(C_6H_5COOH)_2$	1114.0(10)[a]	6224	2
$(HCOOH)_2$	474(12)	2480–5450	6, 7, 9
$HCOOH–HC_2COOH$	291.428(5)	8000	16
$HCOOH–CH_3COOH$	250.44(1)[b]	8000	17
$(AA)_2$	880.6(6)	2485(150)	this work

[a]Errors in parentheses are expressed in units of the last digit. [b]This splitting is for the A state of the internal rotation. A meaningless value of $-136.167(3)$ MHz is reported for the E state.

CONCLUSIONS

In summary, we have assigned the rotational spectra of four isotopologues of the dimer of acrylic acid. The most important results are (i) it is possible to investigate homo dimers of carboxylic acids by rotational spectroscopy; (ii) the observed tunneling splittings of the parent species and three deuterated species have been reproduced by a 3D model with a barrier in the range of theoretical predictions; (iii) to describe the overall effect of the heavy atom modes, the model involves two variables linked to the structural changes between the stationary points of the potential energy surface as obtained *ab initio*; (iv) the reduced mass of the motion changes step by step, so that a flexible model which takes into account these changes is especially suitable for the evaluation of the barrier.

ASSOCIATED CONTENT

S Supporting Information
(1) Complete ref 24; (2) table of transition frequencies; (3) table with B3LYP/6-311++G** optimized geometries for the three minima; (4) table with alternative flexible model fittings. This material is available free of charge via the Internet at http://pubs.acs.org.

AUTHOR INFORMATION

Corresponding Author
walther.caminati@unibo.it
Notes
The authors declare no competing financial interest.

ACKNOWLEDGMENTS

REFERENCES

(1) Gilli, P.; Bertolasi, V.; Ferretti, V.; Gilli, G. *J. Am. Chem. Soc.* **2000**, *122*, 10405−10417.
(2) Kalkman, I.; Vu, C.; Schmitt, M.; Meerts, W. L. *ChemPhysChem* **2008**, *9*, 1788−1797.
(3) Matylitsky, V. V.; Riehn, C.; Gelin, M. F.; Brutschy, B. *J. Chem. Phys.* **2003**, *119*, 10553−10562.

(4) Georges, R.; Freytes, M.; Hurtmans, D.; Kleiner, I.; Auwera, J. V.; Herman, M. *Chem. Phys.* **2004**, *305*, 187−196.

(5) Xue, Z.; Suhm, M. A. *J. Chem. Phys.* **2009**, *131* (054301), 1−14.

(6) Madeja, F.; Havenith, M. *J. Chem. Phys.* **2002**, *117*, 7162−7168.

(7) Ortlieb, M.; Havenith, M. *J. Phys. Chem. A* **2007**, *111*, 7355−7363.

(8) Gutberlet, A.; Schwaab, G. W.; Havenith, M. *Chem. Phys.* **2008**, *343*, 158−167.

(9) Birer, O.; Havenith, M. *Annu. Rev. Phys. Chem.* **2009**, *60*, 263−275.

(10) Riehn, C.; Matylitsky, V. V.; Gelin, M. F.; Brutschy, B. *Mol. Phys.* **2005**, *103*, 1615−1623.

(11) Costain, C. C.; Srivastava, G. P. *J. Chem. Phys.* **1961**, *35*, 1903−1904.

(12) Bellott, E. M., Jr.; Wilson, E. B. *Tetrahedron* **1975**, *31*, 2896−2898.

(13) Martinache, L.; Kresa, W.; Wegener, M.; Vonmont, U.; Bauder, A. *Chem. Phys.* **1990**, *148*, 129−140.

(14) Antolinez, S.; Dreizler, H.; Storm, V.; Sutter, D. H.; Alonso, J. L. *Z. Naturforsch.* **1997**, *52a*, 803−806.

(15) (a) Daly, A. M.; Bunker, P. R.; Kukolich, S. G. *J. Chem. Phys.* **2010**, *132* (201101), 1−3;(b) *ibid.* **2010**, *133* (079903), 1−1.

(16) Daly, A. M.; Douglass, K. O.; Sarkozy, L. C.; Neill, J. L.; Muckle, M. T.; Zaleski, D. P.; Pate, B. H.; Kukolich, S. G. *J. Chem. Phys.* **2011**, *135* (154304), 1−12.

(17) Tayler, M. C. D.; Ouyang, B.; Howard, B. J. *J. Chem. Phys.* **2011**, *134* (054316), 1−9.

(18) Ilyushin, V. V.; Alekseev, E. A.; Chou, Y. C.; Hsu, Y. C.; Hougen, J. T.; Lovas, F. J.; Picraux, L. B. *J. Mol. Spectrosc.* **2008**, *251*, 56−63 and references therein.

(19) Oldani, M.; Bauder, A. *Chem. Phys. Lett.* **1984**, *108*, 7−10.

(20) Bolton, K.; Lister, D. G.; Sheridan, J. *J. Chem. Soc., Faraday Trans. 2* **1974**, *70*, 113−123.

(21) Balle, T. J.; Flygare, W. H. *Rev. Sci. Instrum.* **1981**, *52*, 33−45.

(22) (a) Grabow, J.-U.; Stahl, W. *Z. Naturforsch. A* **1990**, *45*, 1043−1044. (b) Grabow, J.-U. Doctoral Thesis, Christian-Albrechts-Universität zu Kiel: Kiel, 1992. (c) Grabow, J.-U.; Stahl, W.; Dreizler, H. *Rev. Sci. Instrum.* **1996**, *67*, 4072−4084.

(23) Caminati, W.; Millemaggi, A.; Alonso, J. L.; Lesarri, A.; López, J. C.; Mata, S. *Chem. Phys. Lett.* **2004**, *392*, 1−6.

(24) Frisch, M. J.; et al. *Gaussian 03*, Rev. B.01, Gaussian, Inc.: Pittsburgh, PA, 2003.

(25) Boys, S. F.; Bernardi, F. *Mol. Phys.* **1970**, *19*, 553−566.

(26) Pickett, H. M. *J. Mol. Spectrosc.* **1991**, *148*, 371-377.Current versions are described and available from: http://spec.jpl.nasa.gov.

(27) Watson, J. K. G. In *Vibrational Spectra and Structure*; Durig, J. R., Ed.; Elsevier: New York/Amsterdam, 1977; Vol. 6, pp 1−89.

(28) Pickett, H. M. *J. Chem. Phys.* **1972**, *56*, 1715−1723.

(29) Eckart, C. *Phys. Rev.* **1935**, *47*, 552−558.

(30) Kraitchman, J. *Am. J. Phys.* **1953**, *21*, 17−24.

(31) Ubbelohde, A. R.; Gallagher, K. J. *Acta Crystallogr.* **1955**, *8*, 71−83.

(32) See, for example Tang, S.; Majerz, I.; Caminati, W. *Phys. Chem. Chem. Phys.* **2011**, *13*, 9137−9139 and references therein.

(33) (a) Meyer, R.; Ha, T.−K. *Mol. Phys.* **2003**, *101*, 3263−3276;(b) **2005**, *103*, 2687−2698.

(34) A similar approach was chosen earlier for a 2D model for the benzoic acid dimer, see: (a) Meyer, R.; Ernst, R. R. *J. Chem. Phys.* **1990**, *93*, 5518−5532. (b) Stöckli, A.; Meier, B. H.; Kreis, R.; Meyer, R.; Ernst, R. R. *J. Chem. Phys.* **1990**, *93*, 1502−1520.

(35) Manz, J.; Meyer, R.; Pollak, E.; Römelt, J. *Chem. Phys. Lett.* **1982**, *93*, 184−187.

(36) Meyer, R. *J. Mol. Spectrosc.* **1979**, *76*, 266−300.